Distribution of Welding Residual Stresses in Laser Welds with the Nail-head shape

Y. P. Kim, S. M. Joo and H. S. Bang

Abstract

During the laser welding, weldments are suddenly heated and cooled by laser beam of high density energy. This phenomenon gives an occasion to complex welding residual stresses, which have a great influence on structural instability, in laser welds. However, relevant researches on this field are not sufficient until now and residual stress measurements have experimental and practical limitations. From these reasons, a numerical simulation may be attractive in order to solve the residual stress problem. For clarifying the distribution of heat and welding residual stresses in laser welds with the nail-head shape, authors conduct the finite element analysis (two-dimensional unstationary heat conduction & thermal elastic and plastic analysis). From the results, we can confirm the stress concentration occurs at the place of melting line shape changed in laser welds with the nail-head shape.

Key Words : Laser welding, Nail-head shape, Welding residual stresses, Medium carbon steel, Finite element method.

1. Introduction

In recent, the development of new welding methods and its application are expanded. Especially an application of laser welding is remarkable among these new welding methods due to its excellent welding quality with an increase of output power according to the improvement of relevant technology. Its application fields are also diversified in the manufacturing industry including medical engineering; therefore, it is important to understand the mechanical characteristics of laser welds in the product of these fields.

In general, the shape of weld joint is an important parameter to examine mechanical characteristics in the welds. In case of arc welding, this shape has been decided by the angle of groove in weld joint: however, the preparation of groove angle is not needed in laser welding. The shape of laser weld joint is decided by the behavior of fluid dynamics in weld pool. The distinguished shape of laser welds, nail-head shape, is shown according to the circumstances.

Y. P. Kim, S. M. Joo and *H. S. Bang* : Naval architectural engineering, Chosun University, Gwangju, Korea
E-mail : hsbang@mail.chosun.ac.kr

The relevant researches [6, 8, 9] on this fields have been conducted by the numerical analysis and experiment, which have the experimental and practical limitations, to know the condition of mechanical characteristics on the surface of laser welds, but there is no enough to understand the characteristics in laser welds section. So, authors give an attention to the mechanical characteristics in the section of laser welds and we conduct the finite element analysis in order to determine the distribution of heat and welding residual stresses in laser welds with the nail-head shape.

2. Finite element analysis

2.1 Theory of two-dimensional unstationary heat conduction & thermal elastic and plastic analysis

The spatial and temporal temperature distribution satisfies the governing equation for two-dimensional unstationary heat conduction. The heat conduction problem of the solid is formulated as finite element method by using Galerkin method. As a boundary condition in heat analysis, the heat conduction in the model and heat transfer to the atmosphere is considered. An unstationary heat conduction problem is finally described as a following equation (1).

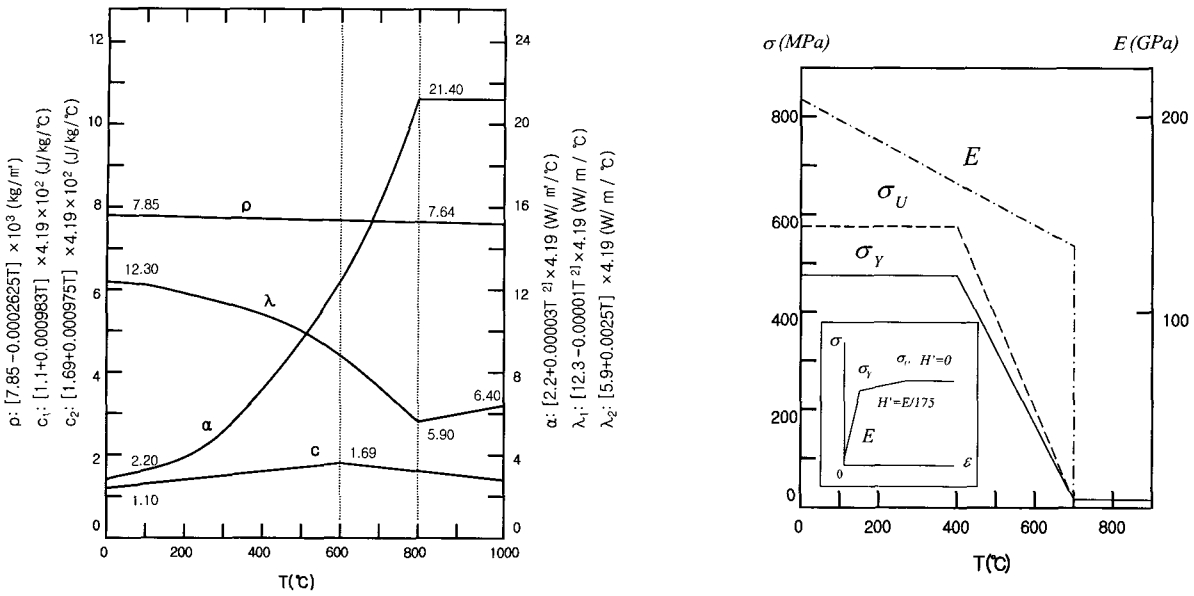

(a) Physical property (b) Mechanical property

Fig. 1 Temperature dependency of physical properties and mechanical properties [1, 2].

$$[K]\{\phi\} + [C]\left\{\frac{\partial \phi}{\partial t}\right\} = \{F\} \quad (1)$$

$[K]$: heat conductivity matrix
$[C]$: heat capacitance matrix
$\{F\}$: heat flow vector at the nodal point

For the thermal elastic and plastic analysis, total strains are considered as the sum of elastic strain (ε^e), plastic strain (ε^p) and thermal strain (ε^t).

$$\varepsilon = \varepsilon^e + \varepsilon^p + \varepsilon^t \quad (2)$$

2.2 Condition of numerical analysis

In this study, the welding heat source is assumed as an instantaneous heat source. Two dimensional four-node isoparametric elements are used to find the value at the node and element as well as any integral point. Medium carbon steel (JIS S45C) has been used for the material of numerical analysis. Fig. 1 shows the physical and mechanical property of the material, which are depending on the temperature.

The material is assumed as an isotropic material. The work-piece is initially at 20℃. Convective flows in the weld pool, vaporization in the keyhole and radiation heat transfer are not considered. In order to analyze the heat conduction and two-dimensional thermal elastic and plastic problem, a self-developed finite element program is used. This program has been verified to provide the accurate result of simulation in the case of arc welding [3, 4]. To increase the accuracy of analysis, equation (3) and (4) adopted in the established researches [5, 6] has been used in combination. Laser welding condition is shown in Table 1.

$$P = P'\exp(-\alpha L) \quad \text{: Beer-Lambert's law [6]} \quad (3)$$

P : beam power reaching a depth L (kW)
P' : incident power
α : absorption coefficient (m^{-1})

$$Q = \eta_L \frac{P}{V} \quad [5] \quad (4)$$

Q : weld heat input (kJ/cm)
P : laser power at the work piece (kW)
V : weld travel speed (cm/sec)
η_L : laser welding efficiency [7]

Table 1 Laser welding condition

Type of Laser	CW Nd:YAG Laser
Beam power	3.3 kW
Focal depth	0 mm
Travel speed	1.25 cm/sec

The schematic mesh division and principle dimensions of the model for analysis are shown in Fig. 1. The number of nodes and elements is 4029 and 3900 respectively. The minimum size of an elements is 0.1mm× 0.1mm.

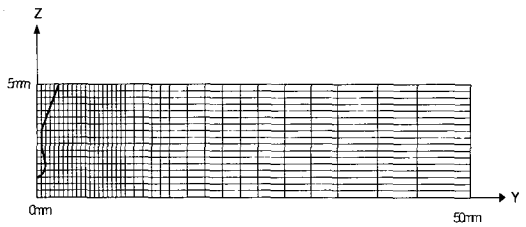

Fig. 2 Schematic mesh division (2-D ½ Model)

Boundary condition for thermal elastic and plastic analysis is shown in Fig. 3.

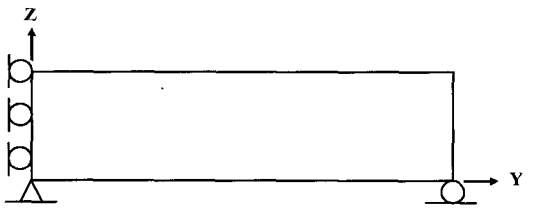

Fig. 3 Boundary condition for thermal elastic and plastic analysis

3. Simulation results and discussion

3.1 Result of heat conduction analysis and discussion

To investigate the simulation results, the thermal and mechanical view lines are adopted in the direction of width and thickness as shown in Fig. 4 respectively.

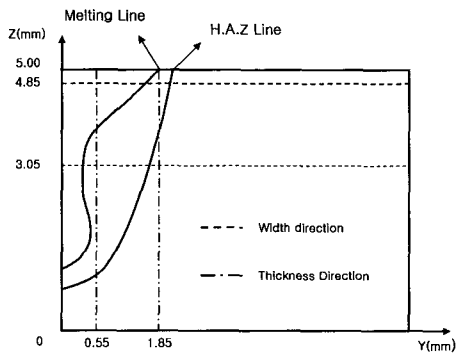

Fig. 4 Thermal and mechanical view lines

Temperature distribution in weld metal and heat affected zone is shown in Fig. 5 at the view lines (z=4.85 ㎜, z=3.05㎜) first. In the Fig. 5 (a), the extreme temperature change is observed in weld metal and heat affected zone at the top. The cooling rates in weld metal and heat affected zone are different each other. The cooling rates at the middle (Fig. 5 (b)) are similar in weld metal and heat affected zone. In order to estimate the difference of cooling rates between top and middle, details on the cooling rates in weld metal and heat affected zone are shown in Fig. 6.

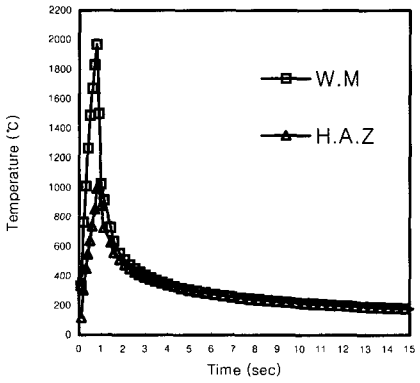

(a) z=4.85mm

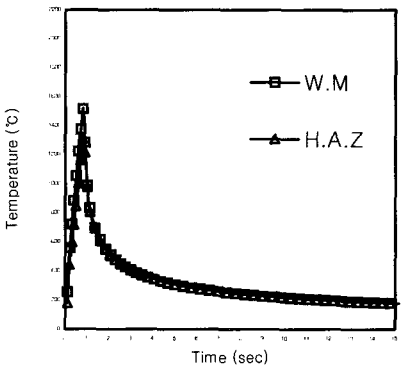

(b) z=3.05mm

Fig. 5 Temperature distribution in W.M and H.A.Z

From the investigation on Fig. 6, it is known that the cooling rates at the top are more rapid than coo ling rates at the middle.

That is considered because a cooling at the top is depending on the heat conduction in the material inside and heat transfer to the atmosphere, but there is no heat transfer phenomenon at the middle.

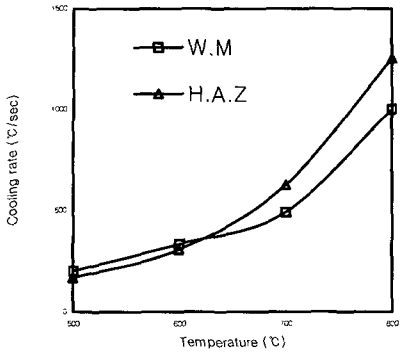

(a) z=4.85mm

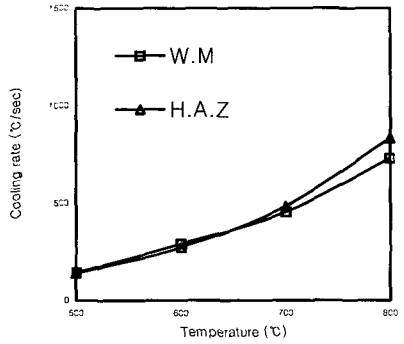

(b) z=3.05mm

Fig. 6 Cooling rates in W.M and H.A.Z

That is considered because a cooling at the top is depending on the heat conduction in the material inside and heat transfer to the atmosphere, but there is no heat transfer phenomenon at the middle.

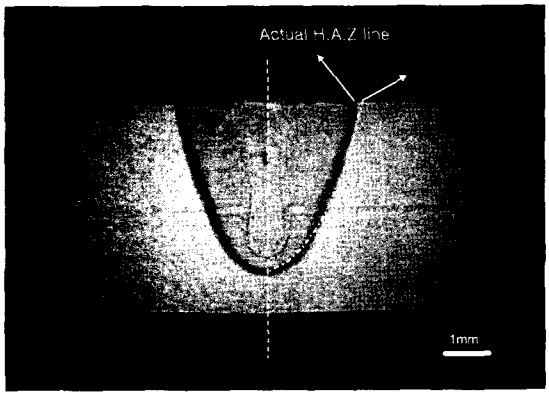

Fig. 7 Comparison between experiment and simulation on the H.A.Z line

The comparison between experiment and simulation to the H.A.Z line is illustrated in Fig. 7. As shown in the figure, above simulation result is well in accord with the experiment result.

3.2 Result of thermal elastic and plastic analysis and discussion

The distribution of welding residual stresses along the width direction is shown at the top (z=4.85mm) and middle (z=3.05mm) in Fig. 8. From this figure, it is known that the width of distribution of maximum welding residual stresses is formed narrowly. That is considered due to narrow heat affected zone. The maximum value of welding residual stress is represented at the adjacent area of heat affected zone to the base metal.

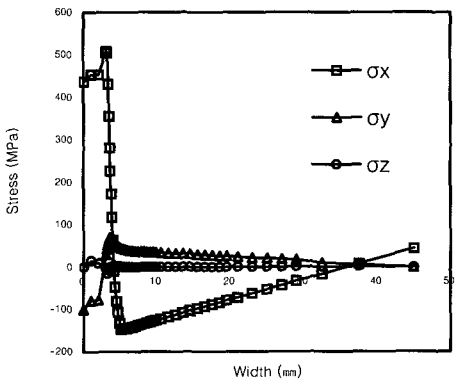

(a) z=4.85mm

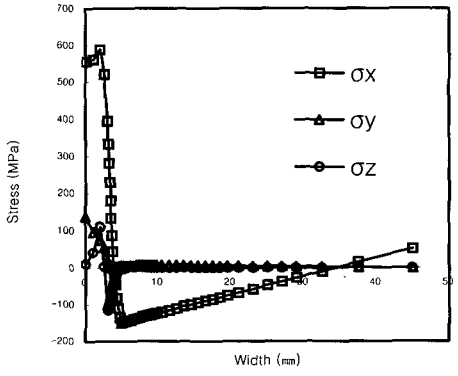

(b) z=3.05mm

Fig. 8 Welding residual stresses along the width direction

The specific characteristics of distribution of welding residual stresses, the component of residual stress (σ_y) in width direction, is different between top and middle. That is considered due to different cooling rates between top and middle. This result is similar with established research result [8].

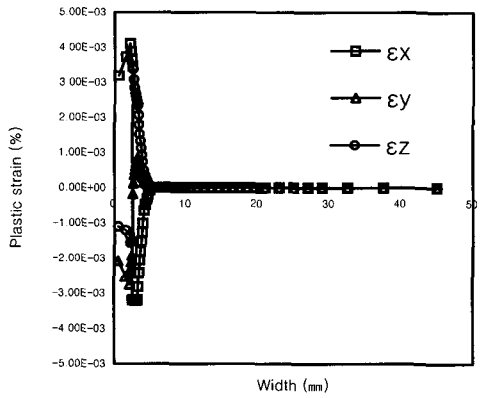

(a) z=4.85mm

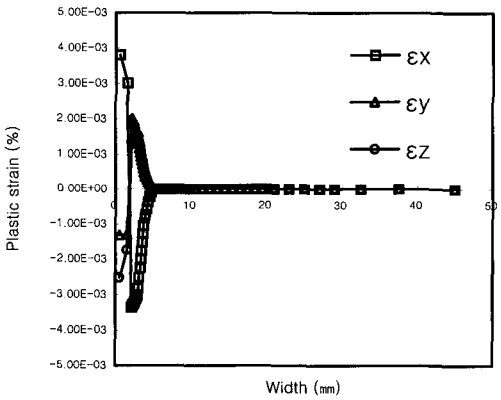

(b) z=3.05mm

Fig. 9 Plastic strain along the width direction

The distribution of plastic strains at the same view lines with welding residual stresses is shown in Fig. 9. The component of plastic strain in thickness direction (ε_z^p) is large relatively. That is considered due to small restraint factor in thickness direction. Corresponding to this phenomenon σ_z is smaller than other stress components.

The mechanical characteristics of welds to the thickness direction is observed at the y=0.55mm and y=1.85mm. The distribution of welding residual stresses and plastic strains along the thickness direction are shown in Fig. 10 and Fig. 11 respectively. It is confirmed that the stress concentration is occurred at the place of melting line shape changed in laser welds with the nail-head shape. The distribution of residual plastic strain represents the similar tendency with the distribution of welding residual stresses.

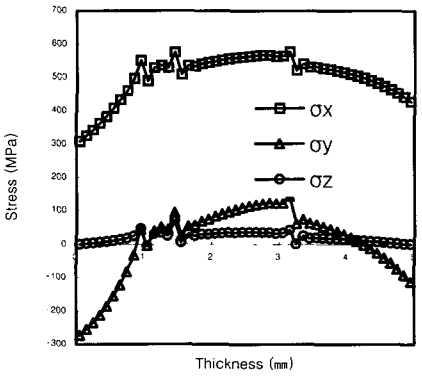

(a) y=0.55mm

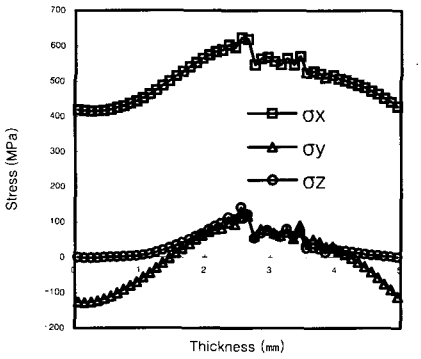

(b) y=1.85mm

Fig. 10 Welding residual stresses along the thickness direction

Therefore, these mechanical characteristics in laser welds with the nail-head shape have to be considered at the design stage of weld joint when the partial penetration welding is applied, especially to the material containing alloy elements and impurities (S and P, etc).

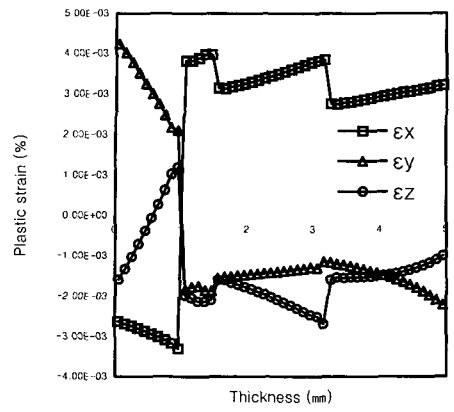

(a) y=0.55mm

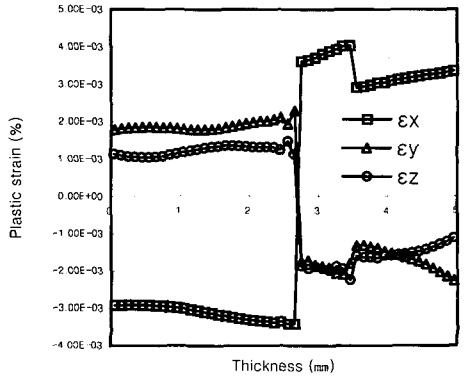

(b) y=1.85mm

Fig. 11 Plastic strain along the thickness direction

4. Conclusion

In this study, authors conduct the heat conduction and thermal elastic and plastic analysis in order to investigate the mechanical behavior in laser welds with the nail-head shape. We can obtain the following results;

1. The cooling rates at the top are more rapid than the cooling rates at the middle. That is due to different thermal boundary conditions between top and middle.

2. According to the narrow heat affected zone of laser welds, the width of distribution of maximum welding residual stresses is formed narrowly. The maximum value of welding residual stress is represented at the adjacent area of heat affected zone to the base metal. The specific characteristics of distribution of welding residual stresses, the component of residual stress (σ_y) in width direction, is different between top and middle. That is considered as an influence of result 1.

3. The stress concentration occurs at the place of melting line shape changed in laser welds with the nail-head shape. These mechanical characteristics have to be considered at the design stage of weld joint when the partial penetration welding is applied.

Acknowledgments

This work was supported by the Brain Korea 21 project in 2002.

References

1. E. A. Brandes and G. B. Brook : Smithells metal reference book, *Butterworth-Heinemann*, (1992), pp. 14–27-14–41, pp. 22–100-22–103
2. D. R. Lide and H. P. R. Frederikse : CRC handbook of chemistry and physics, *CRC press (National Institute of Standards and Technology)*, (1995-1996), pp. 12–176, pp.12–190
3. H. S. Bang and Y. C. Kim : Analysis on the three-dimensional unstationary heat conduction on the welding of thick plate by F. E. M., *Journal of the Korean Welding Society*, Vol. 9, No. 2 (1991), pp. 37-43
4. H. S. Bang : Study on the mechanical behavior of welded part in thick plate, *Journal of the Korean Welding Society*, Vol. 10, No. 4 (1992), pp. 250-258
5. K. W. Carlson : The role of heat input in deep penetration laser welding, *ICALEO*, (1985), pp. 49-57
6. M. R. Frewin and D. A. Scott : Finite element model of pulsed laser welding, *Welding Journal*, Vol. 78, No. 1 (1999), pp. 15s-22s
7. A. Kaplan : A model of deep penetration laser welding based on calculation of the keyhole profile, *J. Phys. D : Appl. Phys.*, Vol. 27, No. 9 (1994), pp. 1805-1814
8. C. Carmignani, R. Mares and G. Toselli : Transient finite element analysis of deep penetration laser welding process in a single pass butt-welded thick plate, *Comput. Methods Appl. Mech. Eng.*,Vol. 179 No. 3 (1999), pp. 197-214
9. H. S. Bang, Y. P. Kim, S. Katayama, W. S. Chang and C. W. Lee : The weldability and mechanical behavior of medium carbon steel in CW Nd:YAG laser welding, *International Journal of KWS*, Vol. 2, No. 1 (2002), pp. 15-20